A 2D asymmetric exclusion model for granular flows

C. JOSSERAND

The James Franck Institute, The University of Chicago
5640 South Ellis Avenue, Chicago, Illinois 60637, USA
Argonne National Laboratory - 9700 South Cass Avenue, Argonne, IL 60439, USA

Abstract. – A 2D version of the asymmetric exclusion model for granular sheared flows is presented. The velocity profile exhibits two qualitatively different behaviors, dependent on control parameters. For low friction, the velocity profile follows an exponential decay while for large friction the profile is more accurately represented by a Gaussian law. The phase transition occurring between these two behaviors is identified by the appearance of correlations in the cluster size distribution. Finally, a mean-field theory gives qualitative and quantitative good agreement with the numerical results.

Introduction. – Among the numerous problems dealing with granular materials, one of the most challenging is granular sheared flow [1-3]. Thus, although granular materials might exhibit solid, liquid or gas-like properties [1], the granular flows cannot be described simply. Granular sheared flow arises in many different contexts such as pipe flow, pyroclastic flows [4], or even traffic jams [5]. Experiments performed in 2D and 3D geometries show surprising velocity profiles. First, the flow occurs only in a sheared region whose width is typically on the order of ten particle sizes (the shear zone). Also, velocity profiles appear to behave differently in 2 and 3 spatial dimensions. The velocity decreases exponentially with the distance to the wall in 2D with a small Gaussian correction [6], while in 3D the profile may appear almost purely Gaussian [7]. The goal of this paper is to present a two-dimensional "toy model" where the velocity profile evolves correspondingly from an exponential-like form to an almost Gaussian form. The model consists of vertically coupled layers. Each layer follows the well-known asymmetric exclusion (ASEP) model. In one dimension, the ASEP model has been widely studied and, under certain conditions, exact solutions have been found using the infinite dimension matrix method [8]. However, to our knowledge, very little is known concerning 2D ASEP model. The numerical simulations will in fact show a cross-over between an exponential velocity profile and a Gaussian velocity profile when the control parameter crosses the value $1/2$. This could be interpreted as a phase transition in infinite-size systems, as the study of the clusters size distribution will indicate. Finally a mean-field approach will be developed for the low values of the control parameter.
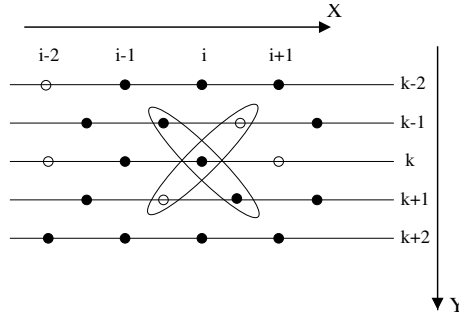
Fig. 1. – 2D lattice with sites (circles) at time t_n: the white circles represent the empty sites or holes, while the black circles represent particles. The motion of the particle located at the position (i, k) is determined as indicated by the motion of its four closest neighbors on rows L_{k+1} and L_{k-1}.

The model. – The 1D ASEP model with periodic boundary conditions describes a one-dimensional lattice of N sites, where each site i ($1 \leq i \leq N$) is either occupied by a particle or empty. During the time interval dt, each particle has a probability dt of jumping to the adjacent site to its right if that site is empty. Our 2D model has a simplified dynamics since the time is now discretized ($t_n = n$). Each layer is a one-dimensional lattice of N sites, with periodic boundary conditions. The layers are labeled L_k ($k \geq 0$). Each site is either occupied or empty and the density along each layer is set to be constant ($= \rho$). A shift of one half of the grid spacing is applied between consecutive layers, so that for k even i is an integer and for k odd, i is a half-integer (see fig. 1). The 2 D lattice is composed of an infinite number of layers occupying the half-space $y \geq 0$. At time t_n, each particle has a probability $P_{i,k}(t_n)$ of hopping to the right. The quantity $P_{i,k}(t_n)$ is determined by the dynamics of the four nearest neighbors of the site (i, k): two in the row L_{k-1} at time t_n and two in the row L_{k+1} at time t_{n-1}. $P_{i,k}(t_n)$ is simply proportional to the number of these neighbors that are moving with a proportionality coefficient α. This linear law accounts for the additionability of the constraints for low stresses. In addition, the exclusion principle imposes that the particle cannot jump to an occupied site. However, if the particle on site $(i + 1, k)$ is jumping to its right at time t_n, then the particle on site (i, k) is allowed to move. If $Q_{i,k}(t)$ is the characteristic function of the motion for the site (i, k) at time t ($Q_{i,k}(t) = 1$, if there is a particle at time t that is jumping from site (i, k), and is zero otherwise) the equation for $P_{i,k}(t_n)$ reads

$$P_{i,k}(t_n) = \alpha(Q_{i-1/2,k-1}(t_n) + Q_{i+1/2,k-1}(t_n) + Q_{i-1/2,k+1}(t_{n-1}) + Q_{i+1/2,k+1}(t_{n-1})). \quad (1)$$

For consistency, if the right-hand side of the formula (1) is bigger than 1, then we define $P_{i,k}(t_n) = 1$. Such a rule defines an abrupt cut-off and smoother behaviors might be considered for large α. Eventually, our boundary condition will represent a moving wall situated at $k = -1$: all the sites of L_{-1} are filled and are moving at each time step. No boundary condition is required for $k = \infty$. The velocity $V_k(t_n)$ is defined as the probability that a particle located on row L_k moves at time t_n. Then, the mean value of the velocity on row L_k is denoted $V(k)$ and defines the velocity profile.

The only control parameter of the dynamics is α. Experimental observations suggest that ρ should be taken close to 1. It appears from the simulations that the dependence on ρ is trivial, and we consider results for $\rho = 0.9$. On the other hand, α reveals how much a moving particle pushes on its neighbors. Therefore, it has to be a (non-trivial *a priori*) function of the material properties such as friction, shape of the grains, their roughness, etc.... Notice that large α represents strong interaction between the layers.
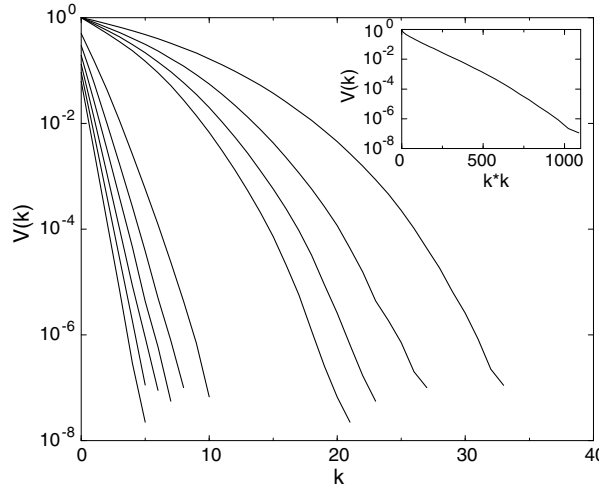
Fig. 2. – Velocity profile for the density $\rho = 0.9$ for different values of the control parameter α. α increases from 0.2 to 0.65 in increments of 0.05 as the curves are plotted from the left to the right. For α smaller than one half the profile is almost exponential and it is far from exponential for $\alpha \geq 0.5$. The insert shows the velocity profile for $\alpha = 0.65$ as a function of k^2. It shows that the profile is better approximated by a Gaussian law, particularly for the low values of k. The number of sites per row is 20000 and the average is computed over 4000 time iterations for 5 different initial conditions for each α.

The model does not allow exchange of particles from one row to another (along the y-direction). This strong constraint is in opposition with the experimental observations, where the density profile seems to reach a steady state where the exchanges between rows just balance. We assume in fact in this model that this interchange of particles is not relevant compared to the friction effects. We also checked that by imposing a reasonable density profile from the moving boundary to the bulk, the qualitative results of the model are not affected. The model exhibits also asymmetric rules since the actions of the upper layer (at time t_n) and the lower layer (at time t_{n-1}) are not simultaneous. In this model, the motion is propagated from the wall to the layers (at time t_n), while the effect of the layer $k + 1$ on the layer k consists in facilitating the motion of the beads, if the particles of the layer $k + 1$ were moving (at time t_{n-1}). In addition, such rules are easier to implement numerically than the simultaneous processes. Moreover, we have performed a few numerical tests to check how this asymmetry affects the results: the rapid decrease of the velocity makes, in fact, the action of the lower level almost negligible and the simulations had the same qualitative features.

Numerical results. – Figure 2 shows different velocity profiles for $\rho = 0.9$ and α increasing from 0.2 to 0.65. For $\alpha \geq 1/2$, an abrupt change in the velocity profile is observed. In fact, we can expand the logarithm of the velocity in a Taylor series:

$$\ln(V(k)) = a + b \cdot k + c \cdot k^2 + d \cdot k^3.... \tag{2}$$

We remark that the three first terms on the right-hand side of (2) give a qualitatively good approximation of the velocity profiles. It corresponds to a Gaussian fit of the profile. However, the ratio b/c indicates the typical width for which the quadratic term becomes of the same order as the linear one. For $\alpha < 0.5$ this ratio is of order of hundreds, *i.e.* much larger than the shear width and the dynamics can be considered almost purely exponential. On the other
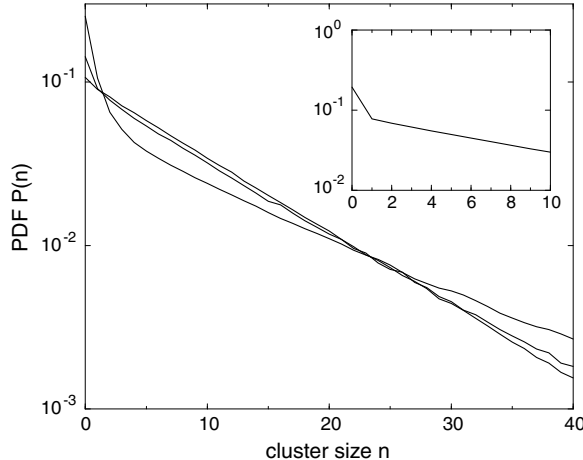
Fig. 3. – The probability distribution function of the cluster size for different values of α and k, and for $\rho = 0.9$. The straight line corresponds to $P_0(n)$ and is $P(n)$ for $\alpha = 0.45$ and $k = 1$. The other two PDF shown are for values of α larger than α_c. The one that is maximum for $n = 0$ is for $\alpha = 0.5$ and $k = 1$, while the next highest is for $\alpha = 0.6$ and $k = 4$. Notice that they show Poisson-like tails at large n, with different slopes. Insert: for $\alpha = 0.49$ and $k = 1$, the PDF differs from $P_0(n)$ only at $n = 0$.

hand, the ratio b/c becomes of the order of 1 when α crosses the critical value $\alpha_c = 0.5$, so that one can approximate the velocity profiles for $\alpha > \alpha_c$ with a Gaussian centered near the row $k = 0$. Such property appears clearly in the insert of fig. 2, where the velocity profile for $\alpha = 0.65$ as a function of k^2 is shown. Notice that for small k ($k^2 < 500$), the logarithm of the velocity is almost linear in k^2, so that one can consider that the velocity profile is Gaussian at least near the wall.

The instantaneous velocity $V_k(t)$ shows also different behaviors whether α is larger or smaller than α_c. Thus, for $\alpha \geq 0.5$, transitory dynamics occur for small time ($t_n < 100$) until the velocity reaches a stationary behavior. Such transitory states cannot be seen for α smaller than 0.5.

In order to investigate more carefully the transition occurring at $\alpha = \alpha_c$, as well as the velocity profiles, a simplified version of the model is introduced. It exhibits the same properties as the model explained above, and can be more easily studied analytically. It consists of neglecting the effect of the row L_{k+1} on the dynamics in row L_k. The model breaks again (and more strongly) the symmetry along the y-direction. However, experimentally, the sheared flows exhibit a spontaneous symmetry breaking as well. A transition from exponential to Gaussian velocity profile occurs in the same way for this simplified model at $\alpha = \alpha_c$. Notice that α_c corresponds to the value of α at which the probability to move becomes 1 if the two neighbors above are moving (the exclusion condition still holds).

We define $P(n)$ as the probability that, given a hole, the next hole on its right is located after n filled sites. $P(n)$ gives the probability distribution function (PDF) for the size of the clusters (if two consecutive sites are empty, it is considered as a cluster of size 0). A priori, the function $P(n)$ depends on ρ, α and the row number k. However, if we consider that the particles are placed randomly on the sites with a density ρ (as do the initial conditions), one obtains the Poisson distribution $P_0(n) = (1 - \rho)\rho^n$. As shown in fig. 3, for $\alpha < \alpha_c$, $P(n)$ corresponds almost exactly to $P_0(n)$ for any k and α. Therefore, at each time step, the particles are distributed on the sites as if they were randomly placed with density ρ. On the
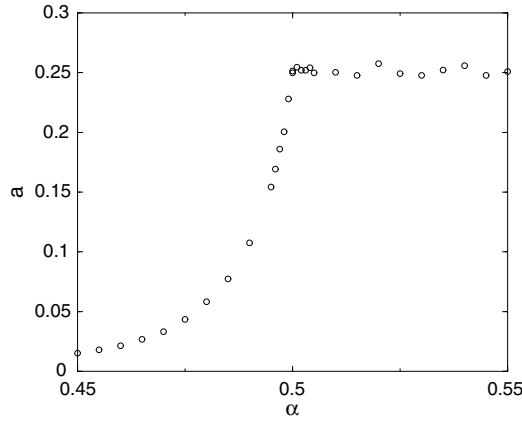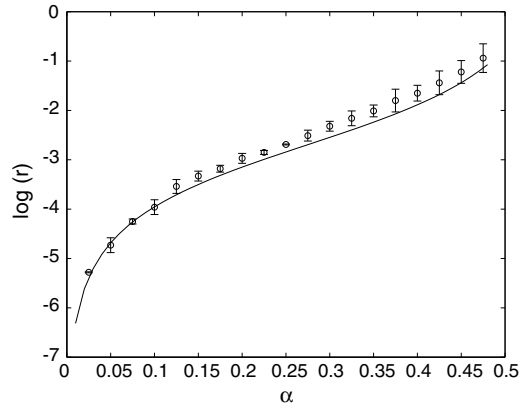
Fig. 4

Fig. 5

Fig. 4. – The density of holes a as a function of α near the phase transition ($\alpha = \alpha_c = 0.5$). a is approximately constant for $\alpha > \alpha_c$ and exhibits a critical exponent of $2/3$ for $\alpha \leq \alpha_c$.

Fig. 5. – $\log(r(\rho, \alpha))$ obtained by numerical simulation (circles) for $\rho = 0.9$ compared to the mean-field approximation $\log(V(1)/V(0))$ (line). $\log(r)$ is computed by a Gaussian fit of the numerical results. The error bars have been evaluated by comparing it with an exponential fit.

other hand, for $\alpha \geq \alpha_c$, the function $P(n)$ differs from $P_0(n)$ in that the small size clusters are more frequent, while large clusters follow a Poisson-like law. In this case, $P(n)$ does not vary as α increases for a given row, but changes as the row number increases: the bigger k, the closer $P(n)$ approaches $P_0(n)$.

When α approaches α_c the PDF differs slightly from $P_0(n)$; for instance, for $k = 1$, we can expand $P(n)$ in the form (see insert of fig. 3)

$$P(n) = a\delta_{n,0} + (1 - a)\rho_{\mathrm{eff}}^n (1 - \rho_{\mathrm{eff}}),$$

with $\rho_{\mathrm{eff}} = \rho/(1 - a(1 - \rho))$ (the mean density has to be ρ). Figure 4 shows the evolution of a as a function of α for $\rho = 0.9$. For $\alpha > \alpha_c$, a is a constant since $a = a_c = 0.25 \pm 0.01$ which corresponds to $\rho_{\mathrm{eff}} \sim 0.92$. However, for $\alpha \leq \alpha_c$ we observe that for $a \sim a_c$

$$a_c - a \propto (\alpha_c - \alpha)^\nu$$

and we found $\nu \sim 2/3$. Therefore, we identify the behavior of the system when α reaches α_c as a phase transition. Notice that when α increases above α_c, the PDF shows a more complex behavior since not only the value of $P(0)$ is disturbed, but also a larger range of clusters size (see fig. 3).

Mean-field theory. – As the correlations can be neglected for $\alpha < \alpha_c$, a mean-field approach is appliable. Defining $P^{(k)}(n)$ as the probability that n successive particles are moving on the row L_k (knowing that an empty site is before such a cluster), $P^{(0)}(n)$ can be computed exactly: $P^{(0)}(n) = (2\alpha\rho)^n(1 - 2\alpha\rho)$ and by noticing that $V(0) = \frac{(1-\rho)}{\rho} \sum n P^{(0)}(n)$, we obtain

$$V(0) = \frac{2\alpha(1 - \rho)}{1 - 2\alpha\rho}.$$

It is remarkable that the numerical simulations and this mean-field solution agree within an error of less than one percent. Also, one can write the constitutive relation between $P^{(0)}$ and

$P^{(1)}$:

$$P^{(1)}(n) = \sum_{l=n-1}^{\infty} W(l \to n) P^{(0)}(l) \,, \tag{3}$$

where $W(l \to n)$ is the probability that if a cluster of size l at row $k = 0$ is moving, then a cluster of size n at row $k = 1$ is moving. It follows that

$$W(l \to n) = (1 - \rho)(2\alpha\rho)^n \left((l - n + 1) - (l - n)2\alpha\rho\right), \quad \text{for} \quad l > n \,,$$

$$W(n \to n) = (1 - \rho)\alpha\rho(2\alpha\rho)^{n-1}(2 - \alpha\rho); \quad W(n - 1 \to n) = (1 - \rho)(\alpha\rho)^2(2\alpha\rho)^{n-2} \,,$$

and we obtain for $V(1)$

$$V(1) = \frac{1 - \rho}{\rho} \sum_{n=1}^{\infty} n P^{(1)}(n) = \frac{2\alpha^2\rho(1 - \rho)^2(2 + \alpha\rho(1 - 2\alpha\rho)^2)}{(1 - 2\alpha\rho)^2(1 + 2\alpha\rho)} \cdot$$

Again, this mean-field solution is in good agreement with the numerical results, although not as accurate as for $V(0)$. Unfortunately, the next-order steps, for obtaining the analytical solutions of $P^{(1)}$ and then $V(2)$ are much more complicate. However, one can consider that for the exponential behavior, the knowledge of $V(0)$ and $V(1)$ is sufficient. Then, we can compare the numerical exponential profile with the exponential law predicted by the mean field. We define $r(\alpha, \rho)$ such that for $\alpha < \alpha_c$, the velocity profile obtained numerically is fit by $V(k) = V(0)(r(\alpha, \rho))^k$.

Figure 5 shows $\log(r)$ as a function of α for $\rho = 0.9$, compared with the mean-field r_{mf} solution taken as

$$r_{mf} = \frac{V(1)}{V(0)} = \frac{\alpha\rho(1 - \rho)(2 + \alpha\rho(1 - 2\alpha\rho)^2)}{1 - (2\alpha\rho)^2} \,.$$

Thus, the mean-field approximation, deducing the exponential law from the ratio between the first two velocities, gives a quantitative good approximation of the exponential decay for $\alpha < \alpha_c$. But, for $\alpha \geq \alpha_c$, the mean-field approach fails and we are not able to show analytical results. Although we were able to quantify clusters size correlations for $\alpha \sim \alpha_c$, numerical simulations show correlations along the y-direction as well.

Conclusion. – It can be argued that most of the features of the phase transition comes from the abrupt cut-off made on eq. (1) when the probability $P_{i,k}$ is greater than one. There is no doubt indeed that the transition is due to the possibility of having a probability one to move if all neighbours are already moving. Then, the exclusion property is dominating the dynamics above the transition. But, the features of the phase transition (dynamical exponent, correlations...) do not depend on the details of the regularization chosen for $P_{i,k} > 1$. On the other hand, one has to ask whether it is physically relevant to have situations where $P_{i,k}$ can reach one. Thus, it is not clear that granular flows can be accounted by the model for $\alpha > \alpha_c$. However, we believe that the phase transition exhibited by the model might have interesting features for granular flows. Also, all the interesting behaviors of the dynamics are precisely seen below the transition; for example, the evolution from exponential toward a Gaussian velocity profile appears near but below the transition. For larger α we only observe a wider profile. In this note, we show in fact that the strength of the interaction between the layers can simply explain different velocity profiles. Moreover, according to the model, we would encourage experiments where the friction coefficient of the granular materials would change.

Furthermore, we would like to investigate other applications of this model to various problems such as non-Newtonian flows or molecular frictions.

Finally, notice that the model is based mainly on probabilistic properties of granular flows. Other stochastic approaches have already been proposed in this context [9, 10], although in granular materials there is no justification such as thermal fluctuations for stochastic processes. However, the shape of the grains, and therefore the contact network in granular materials can be considered as random variables (this has been argued for the chain forces in static bead pile [11]). Additionally, the motion of the particles in shear flows changes the configuration of the contact network of the system. These different properties might give robust confidence for such a probabilistic approach.

$$***$$

REFERENCES

[1] Jaeger H., Nagel S. and Behringer R., *Rev. Mod. Phys.*, **68** (1996) 1259.
[2] Rajchenbach J., in *Physics of Dry Granular Media, NATO ASI Ser. E*, **350** (1998) 421.
[3] Kadanoff L., *Rev. Mod. Phys.*, **71** (1999) 435.
[4] Straub S., *Geol. Rundsch.*, **85** (1996) 85.
[5] Ben-Naim E., Krapivsky P. L. and Redner S., *Phys. Rev. E*, **50** (1994) 822.
[6] Veje C., Howell D., Behringer R., Schöllmann S., Luding S. and Herrmann H., in *Physics of Dry Granular Media, NATO ASI Ser. E*, **350** (1998) 237; Veje C. T., Howell D. W. and Behringer R. P., *Phys. Rev. E*, **59** (1999) 739.
[7] Mueth D. M., Debregeas G. F., Karczmar G., Jaeger H. M. and Nagel S. R., preprint (1999).
[8] Derrida B., Evans M., Hakim V. and Pasquier V., *J. Phys. A: Math. Gen*, **26** (1993) 1493.
[9] Pouliquen O. and Gutfraind R., *Phys. Rev. E*, **53** (1996) 552.
[10] Debregeas G. and Josserand C., cond-mat/9901336.
[11] Liu C., Nagel S., Schecter D., Coppersmith S., Majumdar S., Narayan O. and Witten T., *Science*, **269** (1995) 513; Mueth D. M., Jaeger H. M. and Nagel S. R., *Phys. Rev. E*, **57** (1998) 3164.